Influence of Saccharin and 2-Butyne-1,4diol on the Electrodeposition of Zn-Ni Alloys Coatings: Application of a Mixture Design

Hawa Bendebane[1]*, Salima Bendebane[2], Samia Amirat[1] and Rabah Rehamnia[1]

[1]*Department of Chemistry- Laboratory LNCTS UBM, Annaba, Algeria*
[2]*Laboratory LOMOP, Higher National School of Mines and Metallurgy Amar Laskri, Annaba, Algeria*
*Corresponding author: bendebanehawa@yahoo.fr

Received 19/06/2023; accepted 02/12/2023
https://doi.org/10.4152/pea.2025430202

Abstract
Herein, electrodeposition of Zn-Ni alloy thin films on CS substrates under various conditions, from sulfate baths containing $Na_3C_6H_5O_7$, $C_7H_5NO_3S$, and 2-butyne-1,4diol, was studied. So as to have the best bath composition, a mixture design application was examined. The best obtained composition was: 0.3 M $Na_3C6H_5O_7^-$, 0.1 g/L $C_7H_5NO_3S$ and 0.1 g/L 2-butyne-1,4-diol, for theoretical and experimental responses of 215.22 and 221.60 HV, respectively. Zn-Ni coating morphological properties and composition were examined by SEM and EDS. It was found that, on optimal conditions, a significant decrease in the grain size occurred. The deposits were homogeneous, uniform, compact and fine-grained, without any pores at the surface.

Keywords: 2-butyne-1,4-diol; $C_7H_5NO_3S$; mixture design; $Na_3C6H_5O_7^-$; sulfate acid bath; Zn-Ni electrocoatings.

Introduction•

It is well recognized that composite coatings of a single metal and alloys protect steel against corrosion, by improving its mechanical, physical and/or electrochemical properties. As such, Zn-based alloys have attracted a lot of interest in the last decade [1-9]. Zn-Ni alloy has received more attention, due to its high degree of corrosion resistance, mechanical characteristics and thermal stability, compared to Zn only and other Zn alloys coatings [10-17]. Zn-Ni alloy is more toxic than Zn-Cd alloy [18, 19], although it has been widely used in automotive, aeronautic, marine, building and electronics industries [20-22].
In order to improve coating quality, using additives is generally recommended. Generally, a small amount of additives affects the electroplating reaction kinetics, mainly by adsorption or complexation [23, 24]. Therefore, metals and metal oxides electroplating is often performed in baths containing organic additives [25-29].
The present study dealt with Zn-Ni coating electroplating from a sulfate bath. The main goal was to find the best bath composition that would produce coatings

• The abbreviations list is on page 108.

with high quality and hardness. For this purpose, a mixture design method was examined, which provided maximum information on its constituents, their individual influences and possible interactions. This assessment allowed reducing the experiments number, facilitating the study planning and procedures [30, 31]. The desired response depended on the bath components concentration, which were $Na_3C6H_5O_7^-$, $C_7H_5NO_3S$ and 2-butyne-1,4-diol.

Experimental

Material

Low CS, conforming to SAE 1010, ASTM A-366 and QQS-698 standards, was used in this study. CS substrate chemical composition is given in Table 1.

Table 1: Chemical composition of CS substrate.

Element	C	Mn	P	S	Fe
max%	0.13	0.60	0.40	0.05	Remainder

Electroplating

Zn-Ni alloy coatings electrodeposition was carried out in a sulfate acid bath, of which compositions and operating conditions are shown in Table 2. The solution pH was from 4.3 to 4.5. Each experiment was performed in a fresh solution, to avoid problems such as metal ions depletion from the electrolyte.

Table 2: Bath composition and operating conditions.

Composition	Quantity	Operating conditions
$ZnSO_4.7H_2O$	0.10 M	4.3 < pH < 4.5
$NiSO_4.6H_2O$	0.10 M	G = 63.8 mS
Na_2SO_4	0.40 M	T: 30 ± 1 °C
H_2SO_4	0.01M	Stirring speed: 300 rpm
$Na_3C_6H_5O_7$	0.10- 0.30 M	Electrolyte volume: 100 mL = 1 A/dm²
$C_7H_5NO_3S$	0 - 0.30 g/L	e = 15 µm
2-butyne-1,4-diol	0 - 0.30 g/L	

Zn-Ni deposits electrodeposition was performed in a conventional electrochemical cell with two electrodes (cathode and anode), to which constant ddp was applied, using a generator. The procedure was carried out by fixing the following parameters: T of 30±1 ºC, stirring speed around 300 rpm, electrolyte volume of 100 mL, I of 1 A/dm² and thickness of 15 µm. However, $Na_3C6H_5O_7^-$, $C_7H_5NO_3S$ and 2- butyne-1,4-diol concentrations were changed, according to a matrix given by the mixture design (MINITAB 18) (Table 3).

Table 3: Experimental results according to the mixture design.

Std.	$Na_3C6H_5O_7$	$C_7H_5NO_3S$	2butyne1,4diol	Microhardness	Theo microhardness	Relat.	Absol.
2	0.10	0.30	0.10	194.20	198.60	2.22	4.40
10	0.13	0.13	0.23	136.80	164.66	16.92	27.86
8	0.23	0.13	0.13	168.80	182.53	7.52	13.73
1	0.30	0.10	0.10	221.60	215.22	2.96	6.38
6	0.10	0.20	0.20	144.60	156.38	7.53	11.78
9	0.13	0.23	0.13	182.30	163.68	11.37	18.62
3	0.10	0.10	0.30	174.50	163.41	6.78	11.09
7	0.17	0.17	0.17	202.10	162.92	24.05	39.18
4	0.20	0.20	0.10	141.70	158.19	10.42	16.49
5	0.20	0.10	0.20	195.30	196.30	0.51	1.00

Results and discussion

Simplex plot

The simplex plot shows points in the plane space, which are: three at the triangle vertices, for 0.3 M $Na_3C_6H_5O_7^-$, 0.3 g/L $C_7H_5NO_3S$ and 0.3 g/L 2butyne1,4diol pure solutions; three on the triangle sides for the mixtures; and one in the triangle center consisting of the three components in equal proportions. These three complete mixtures had all components, but in different proportions (Fig. 1).

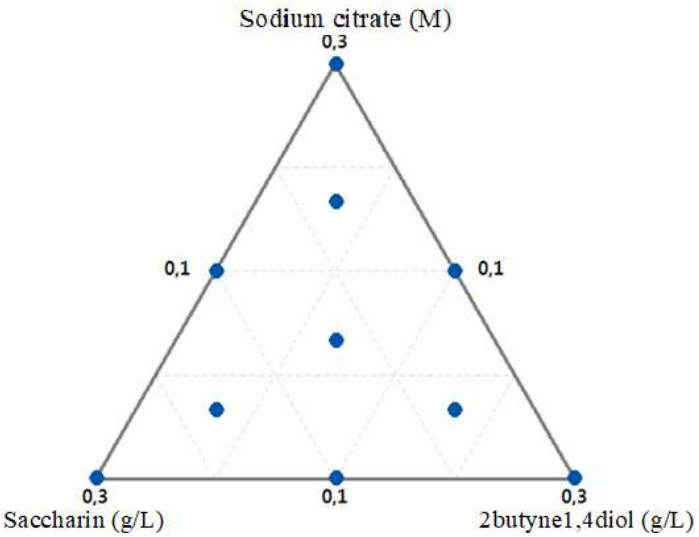

Figure 1: Simplex plot.

Henry's line of residual values

Generally, Henry's line is useful for checking the model normality. It is seen that the points tend to form a line (Fig. 2).

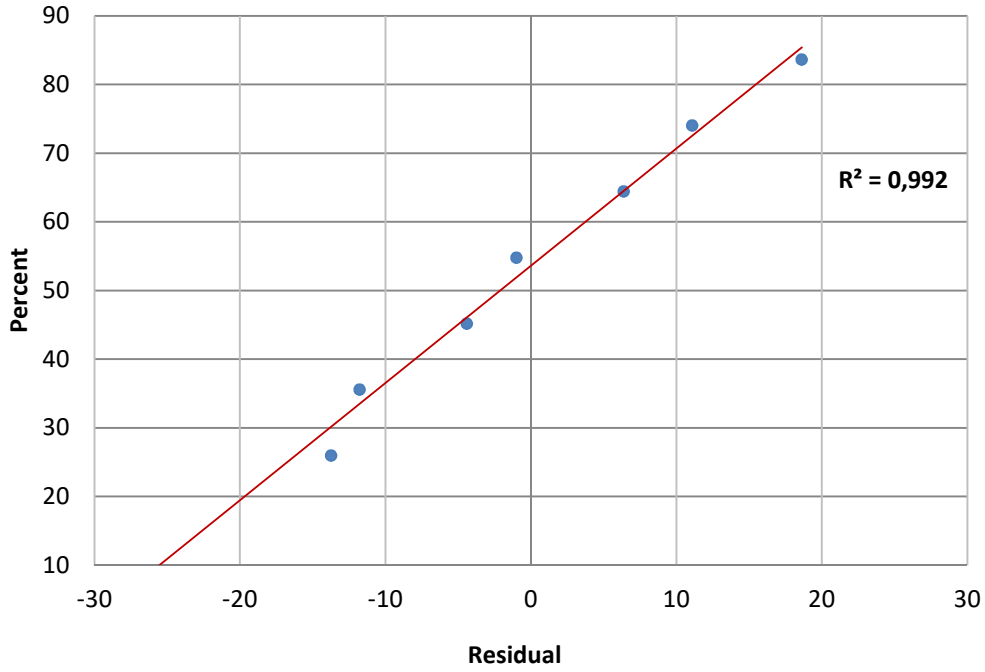

Figure 2: Henry's line of residual values for micro-hardness.

Cox plot

The Cox plot (Fig. 3) presents the evolution of the estimated response by varying the proportion of a single component from a reference mixture, while keeping constant the other components ratio [30]. It consists in representing micro-hardness variations along the Cox axis.

Micro-hardness decreased with increased $C_7H_5NO_3S$ concentrations in the mixture, up to the reference line. On the other hand, beyond this line, an increase in micro-hardness was observed. It was also found that 2-butyne1,4diol presence did not have a remarkable effect on micro-hardness. However, $Na_3C6H_5O_7^-$ had a positive effect on the obtained coatings micro-hardness.

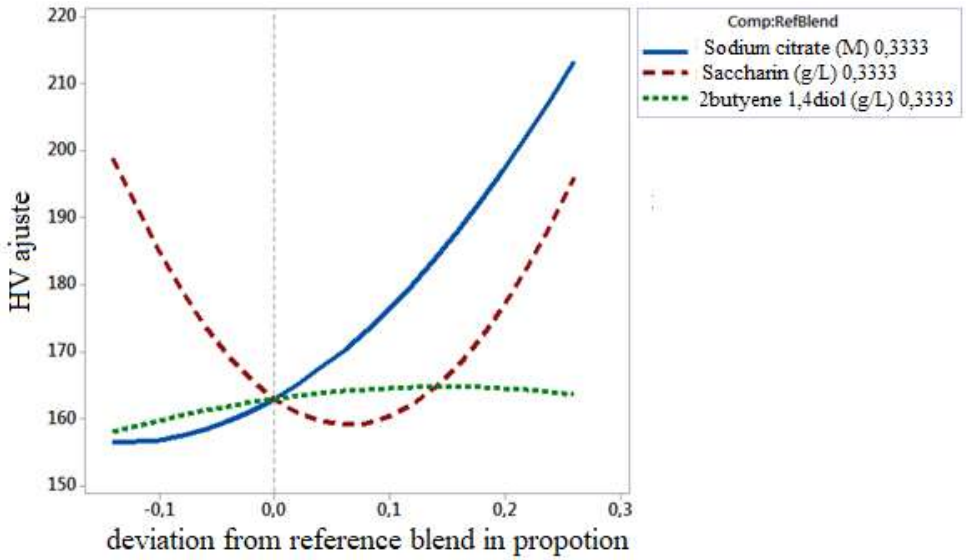

Figure 3: Cox plot.

Mathematical model

The mathematical model applied to the response (Zn-Ni coating micro-hardness) is a quadratic model for three components, with a total of six coefficients for a single response, according to eq. 1.

$$HV = 783.54 \times [Na_3C6H_5O_7^-] + 1016.54 \times [C_7H_5NO_3S] + 283.54 \times [\text{2butyne 1,4diol}] - 4872.22 \times [Na_3C6H_5O_7^-] \times [C_7H_5NO_3S] + 698.23 \times [Na_3C6H_5O_7^-] \times [\text{2butyne 1,4diol}] - 2462.68 \times [C_7H_5NO_3S] \times [\text{2butyne 1,4diol}] \quad (1)$$

Graphics contour and surface response

Simplex contour and response surfaces are shown in Fig. 4. On its left side, $Na_3C6H_5O_7^-$, $C_7H_5NO_3S$, and 2butyne1,4diol contour area and micro-hardness are shown. The best responses are represented by the red contour (>210 HV), which is located at the high level for 0.3 g/L $Na_3C6H_5O_7^-$, and at the low level for 0.1 g/L $C_7H_5NO_3S$ and 2butyne1,4diol each. The response surface represented in a polyhedron (on Fig. 4 right) is a concave triangle shape.

It is seen that microhardness increased with lower $C_7H_5NO_3S$ and 2butyne1,4diol concentrations, and with higher $Na_3C6H_5O_7^-$ content.

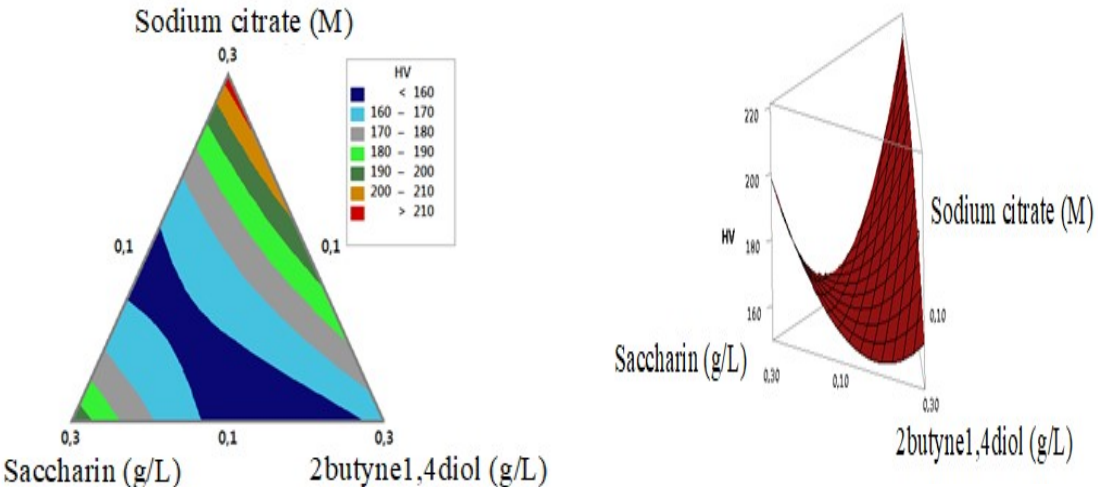

Figure 4: Contour and response surface of a mixture: $Na_3C6H_5O_7^-$, $C_7H_5NO_3S$ and 2butyne 1,4diol.

Optimization

There are many optimization methods. Most of them have been created to deal with the mathematical problem of finding the multi-variable extreme, whether non-linear functions are subject to constraints or not. After several optimizations, the best results are shown in Table 4.

Table 4: Optimal composition of the mixture $Na_3C6H_5O_7^-$, $C_7H_5NO_3S$ and 2butyne 1,4 diol.

Optimal composition			Theoretical response (HV)	Experimental response (HV)
$Na_3C6H_5O_7^-$ (M)	$C_7H_5NO_3S$ (g/L)	2butyne1,4diol (g/L)		
0.30	0.10	0.10	215.22	221.60

Theoretical and experimental responses

The following figure represents the plot of experimental response as a function of theoretical response. From Fig. 5, we can see that the experimental and estimated responses are on the regression line, with a very good value of 0.9846.

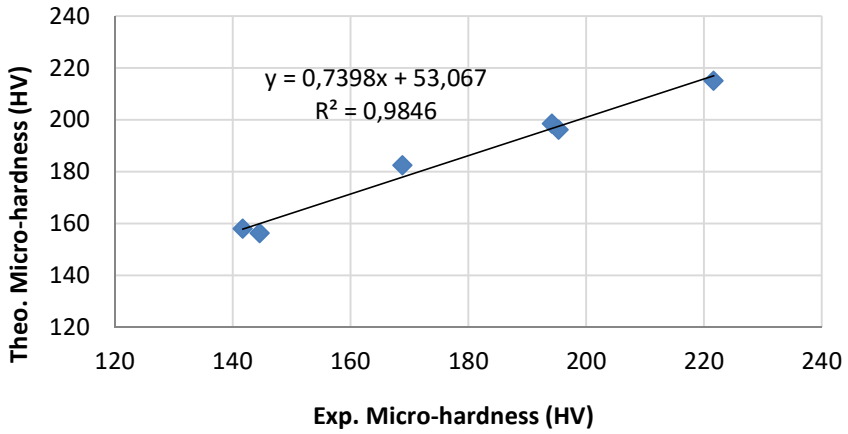

Figure 5: Graphical representation of theoretical responses as a function of experimental responses.

From Table 2, it was confirmed that there was not a significant difference between experimental and theoretical values, which is represented by the relative and absolute incertitudes calculated according to eqs. 2 and 3, respectively.

$$Relative\ incertitude\ (\%) = \left|\frac{\text{Theo.}_{\text{microhardness}} - \text{Exp.}_{\text{microhardness}}}{\text{Theo.}_{\text{microhardness}}}\right| \times 100 \quad (2)$$

$$Absolute\ incertitude\ (\%) = \left|\text{Theo.}_{\text{microhardness}} - \text{Exp.}_{\text{microhardness}}\right| \quad (3)$$

Characterization

SEM analysis

SEM images show that the bath composition influenced the coating quality. Indeed, with $Na_3C6H_5O_7^-$ only (Fig. 6a), a CS non-homogeneous oxidized surface was obtained.

In contrast, the CS surface morphology was improved by $C_7H_5NO_3S$ addition (Fig. 6b), which turned out to be more homogeneous and less oxidized compared than that of Fig. 6a.

By adding $Na_3C6H_5O_7^-$ and 2butyne1,4diol, the obtained deposit formed cracks (Fig. 6c). It is also seen that the grains have a large size and cauliflower shape. The same results were found by [32, 33]. It was found that the best surface in terms of quality and brightness was obtained in the presence of all additives (Fig. 6d).

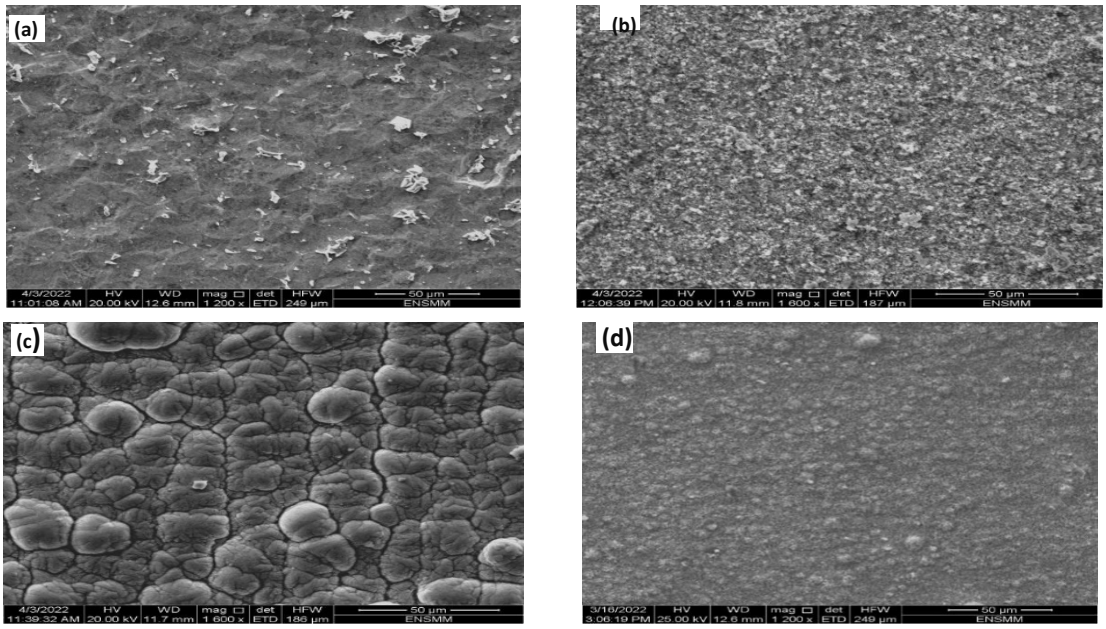

Figure 6: SEM image of Zn-Ni alloys deposited at different baths: **(a)** $Na_3C6H_5O_7^-$; **(b)** $Na_3C6H_5O_7^-$ + $C_7H_5NO_3S$; **(c)** $Na_3C6H_5O_7^-$ + 2butyne1,4diol; and **(d)** $Na_3C6H_5O_7^-$ + $C_7H_5NO_3S$ + 2butyne1,4diol. I = 1A/dm², T = 30 ºC, ss = 300 rpm, $V_{electrolyte}$ = 100 mL and e = 15µm.

EDS analysis

EDS analysis results showed that Zn content of Fig. 7a was lower than that of Fig. 7d, contrary to O. Ni concentration in the deposit varied between 6 and 21%. From literature, it was reported that Zn-Ni coatings ranging from 10 to 15 wt% Ni have better corrosion resistance [34].

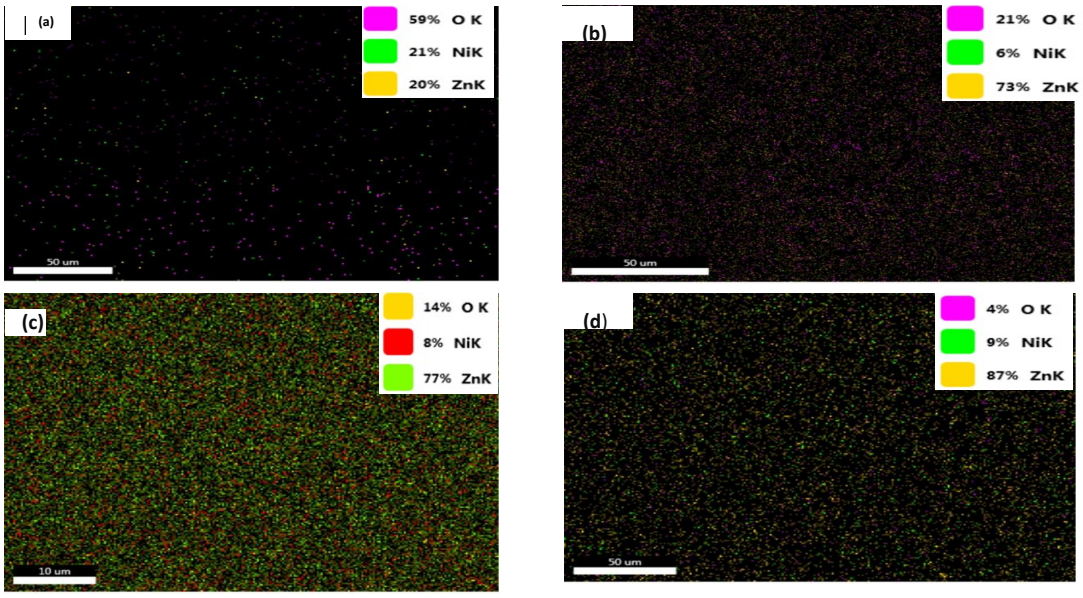

Figure 7: EDS elemental map analysis for **(a)** $Na_3C6H_5O_7^-$; **(b)** $Na_3C6H_5O_7^-$ + $C_7H_5NO_3S$; **(c)** $Na_3C6H_5O_7^-$ + 2butyne1,4diol; and **(d)** $Na_3C6H_5O_7^-$ + C7H5NO3S + 2butyne1,4diol. I = 1A/dm², T = 30 ºC, ss = 300 rpm, V electrolyte = 100 mL and e = 15 µm.

Discussion

These findings are consistent with other previous results, and the change in Zn-Ni alloy coatings quality and micro-hardness is explained by the additive molecules adsorption onto the cathode surface.

It was found, by [11], that $Na_3C_6H_5O_7^-$ effectively stabilizes Zn–Ni alloy plating baths. According to [35], it was found that $Na_3C_6H_5O_7^-$ addition influenced the grains morphology and size.

$C_7H_5NO_3S$ and 2-butyne 1-4 diol organic additives used in this study influenced the obtained coating roughness, by preventing the formation and growth of nodular structures. This finding was also reported by [36- 38].

It was found that O can disrupt the process, due to the formation of $Zn(OH)_2$ precipitate, which inhibits Ni deposition. This result agrees with that of [39], who found that O incorporation into the deposits is probably due to the formation of $Zn(OH)_2$ layer.

Conclusion

This study was focused on the protection of low-CS against corrosion, using electrodeposition as a solution. Zn-Ni coatings were produced from a sulfate bath with 0.1 to 0.3 g/L of both $C_7H_5NO_3S$ and 2-butyne1-4diol (0.1 to 0.3 g/L) as additives, and 0.1 to 0.3 M $Na_3C6H_5O_7^-$ as complexing agent.

The electrodeposition performance of Zn-Ni coating can be improved with the three components blend, by applying the mixture design method. This method employed a quadratic model that considered microhardness as a response to various constituents. A set of experiences and proposed formulations to determine the optimum conditions was herein built, leading to a gray, smooth, uniform, hard and bright coating.

The mathematical model was validated by comparing theoretical and experimental microhardness results. Indeed, the fit was almost perfect, as the linear correlation constant was 0.9846.

Optimization gave a mixture of three components, of which concentrations were 0.3 M $Na_3C6H_5O_7^-$ and 0.1 g/L each $C_7H_5NO_3S$ and 2-butyne1,4diol. This corresponded to a theoretical microhardness of 215.22 HV. Indeed, to confirm and validate the theoretically obtained results, a check for an additional experiment under optimal conditions was performed, and the experimentally obtained microhardness value was 221.60 HV.
From SEM analysis, it was found that the presence of additives played a significant role on the deposit surface morphology and homogeneity.

Acknowledgments
We thank Prof. Rehamnia Rabah Director of the LNCTS Research Laboratory and Dr. Amirat Samia, Head of Chemistry Department, Badji Mokhtar University of Annaba, for providing us with the necessary material resources. The authors thank also the ENSMM-Annaba for the assistance provided in this research, through SEM-EDS analyzes.

Conflict of interest
The authors declare that they have no known competing financial interests or personal relationships that could have appeared to influence the work reported in this paper.

Authors' contributions
Hawa Bendebane: designed the research work; performed the experimental work; carried out data analysis and interpretation; acted as corresponding author. **Salima Bendebane:** contributed to the interpretation of results; made the paper English corrections; improved the quality of the paper. **Samia Amirat:** supervised the work at certain parts. **Rabah Rehamnia:** provided methodology and investigation. All authors read and reviewed the manuscript.

Abbreviations
ASTM: American Society for Testing and Materials
$C_7H_5NO_3S$: saccharine
CS: carbon steel
ddp: potential difference
e: thickness (µm)
EDS: energy dispersive spectroscopy
G = conductivity (mS):
H_2SO_4: sulfuric acid
HV: microhardness unit
I: current density
Na_2SO_4: sodium sulfate
$Na_3C6H_5O_7$: sodium citrate
$NiSO_4.6H_2O$: nickel sulfate hexahydrate
SEM: scanning electron microscopy
Theo: theobromine
Zn-Ni: zinc-nickel alloy
$Zn(OH)_2$: zinc hydroxide
$ZnSO_4.7H_2O$: white vitriol

References

1. Nayana KO,Venkatesha TV, Chandrappa KG. Influence of additive on nanocrystalline, bright Zn–Fe alloy electrodeposition and its properties. Surf Coat Technol. 2013;235:461-468. https://doi.org/10.1016/j.surfcoat.2013.08.003
2. He J, Li DW, He FL et al. A study of degradation behaviour and biocompatibility of Zn—Fe alloy prepared by electrodeposition. Mater Sci Eng C. 2020;117;111295. https://doi.org/10.1016/j.msec.2020.111295
3. He QQ, Zhou MJ, Hu JM. Electrodeposited Zn-Al layered double hydroxide films for corrosion protection of aluminum alloys. Electrochim Acta. 2020;355:136796. https://doi.org/10.1016/j.electacta.2020.136796
4. M. Riđošić, E. García-Lecina, A. Salicio-Paz et al. The advantage of ultrasound during electrodeposition on morphology and corrosion stability of Zn-Co alloy coatings. Transactions of the IMF. Int J Surf Eng Coat. 2020;98:114-120. https://doi.org/10.1080/00202967.2020.1748390
5. Borissov D, Pareek A, Renner FU et al. Electrodeposition of Zn and Au–Zn alloys at low temperature in an ionic liquid. Phys Chem Chem Phys. 2010;12:2059-2062. https://doi.org/10.1039/B919669B
6. Maniam KK, Paul S. Progress in Electrodeposition of Zinc and Zinc Nickel Alloys Using Ionic Liquids. Appl Sci. 2020;10:5321. https://doi.org/10.3390/app10155321
7. Maniam KK, Paul S. Corrosion Performance of Electrodeposited Zinc and Zinc-Alloy Coatings in Marine Environment. Corros Mat Degrad. 2021;2(2):163-189. https://doi.org/10.3390/cmd2020010
8. Loukil N, Feki M. Review—Zn–Mn Electrodeposition: A Literature Review. J Electrochem Soc. 2020;167:022503. https://doi.org/10.1149/1945-7111/ab6160
9. Touazi S, Bučko M, Makhloufi L et al. Zn–Mn alloy coatings electrodeposited from acidic sulfate-citrate bath. Mater Today: Proc. 2022;49:919-924. https://doi.org/10.1016/j.matpr.2021.05.574
10. Anwar S, Khan F, Zhang et al. Optimization of Zinc-Nickel Film Electrodeposition for Better Corrosion Resistant characteristics. Canad J Chem Eng. 2019;97:2426-2439. https://doi.org/10.1002/cjce.23521
11. Anwar S, Zhang Y, Khan F. Electrochemical behaviour and analysis of Zn and Zn–Ni alloy anti-corrosive coatings deposited from citrate baths. RSC Adv. 2018;8:28861-28873. https://doi.org/10.1039/C8RA04650F
12. Beltowska-Lehman E, Ozga P, Swiatek Z et al. Influence of structural factor on corrosion rate of functional Zn–Ni coatings. Cryst Eng. 2002;5:335-345. https://doi.org/10.1016/s1463-0184(02)00045-x
13. Yogesha S, Hegde AC. Optimization of bright zinc-nickel alloy bath for better corrosion resistance. Trans Ind Inst Met. 2010;63:841-846. https://doi.org/10.1007/s12666-010-0128-4
14. Bahadormanesh B, Ghorbani M, Kordkolaei NL. Electrodeposition of nanocrystalline Zn/Ni multilayer coatings from single bath: influences of deposition current densities and number of layers on characteristics of deposits. Appl Surf Sci. 2017;404:101-109. https://doi.org/10.1016/j.apsusc.2017.01.251

15. Bai Y, Wang ZH, Li XB et al. Corrosion behavior of low pressure cold sprayed Zn-Ni composite coatings. J Alloys Comp. 2017;719:194-202. https://doi.org/10.1016/j.jallcom.2017.05.134
16. Roventi G, Cecchini R, Fabrizi A et al. Electrodeposition of nickel–zinc alloy coatings with high nickel content. Surf Coat Technol. 2015;276:1-7. https://doi.org/10.1016/j.surfcoat.2015.06.043
17. Mosavat SH, Shariat MH, Bahrololoom ME. Study of corrosion performance of electrodeposited nanocrystalline Zn–Ni alloy coatings. Corros Sci. 2012;(59)0:81-87.
18. Shams A, Khan F, Zhang YI et al. Zn composite corrosion resistance coatings: What works and what does not work? J Loss Prev Proc Ind. 2021;69:104376. https://doi.org/10.1016/j.jlp.2020.104376
19. Bielawski M. Alternative technologies and coatings for electroplated cadmium and hard chromium. Can Aeronaut Space J. 2010;56:67-80. https://doi.org/10.5589/q11-001
20. Zhai X, Sun C, Li K et al. Composite deposition mechanism of 4,5-dichloro-2-n-octyl-4-isothiazolin-3-one in zinc films for enhanced corrosion resistant properties. J Ind Eng Chem. 2016;36:147-153. https://doi.org/10.1016/j.jiec.2016.01.033
21. Vieira L, Schennach R, Gollas B. The effect of the electrode material on the electrodeposition of zinc from deep eutectic solvents. Electrochim Acta. 2016;197:344-352. https://doi.org/10.1016/j.electacta.2015.11.030
22. Haerens K, Matthijs E, Chmielarz A et al. The use of ionic liquids based on choline chloride for metal deposition: A green alternative? J Environ Manag. 2009;90:3245-3252. https://doi.org/10.1016/j.jenvman.2009.04.013
23. Wasekar NP, Haridoss P, Seshadri SK et al. Influence of mode of electrodeposition, current density and saccharin on the microstructure and hardness of electrodeposited nanocrystalline nickel coatings. Surf Coat Technol. 2016;291:130-140. https://doi.org/10.1016/j.surfcoat.2016.02.024
24. Lokhande A. Studies on surface treatment of electrodeposited Ni–Zn alloy coatings using saccharin additive. J Solid State Electrochem. 2017;(21)9:11. https://doi.org/10.1007/s10008-017-3558-7
25. Lokhande AC, Shelke A, Babar PT et al. Studies on surface treatment of electrodeposited Ni–Zn alloy coatings using saccharin additive. J Solid State Electrochem. 2017;21:2725-2735. https://doi.org/10.1007/s10008-017-3558-7
26. Wu LK, Liu L, Li J, Hu et al. Electrodeposition of cerium (III)-modified bis-[triethoxysilypropyl] tetra-sulphide films on AA2024-T3 (aluminum alloy) for corrosion protection. Surf Coat Technol. 2010;204:3920-3926. https://doi.org/10.1016/j.surfcoat.2010.05.027
27. Moutarlier V, Neveu B, Gigandet MP. Evolution of corrosion protection for sol–gel coatings doped with inorganic inhibitors. Surf Coat Technol. 2008;202:2052-2058. https://doi.org/10.1016/j.surfcoat.2007.08.040
28. Palomino LM, Suegama PH, Aoki IV et al. Electrochemical study of modified cerium–silane bi-layer on Al alloy 2024-T3. Corros Sci. 2009;51:1238-1250. https://doi.org/10.1016/j.corsci.2009.03.012
29. Li X, Deng S, Fu H et al. Synergistic inhibition effect of rare earth cerium (IV) ion and 3, 4-dihydroxybenzaldehye on the corrosion of cold rolled steel in H_2SO_4 solution. Corros Sci. 2009;51:2639-2651. https://doi.org/10.1016/j.corsci.2009.06.047

30. Li X, Deng S, Fu H et al. Synergism between rare earth cerium(IV) ion and vanillin on the corrosion of cold rolled steel in 1.0 M HCl solution. Corros Sci. 2008;50:3599-3609. https://doi.org/10.1016/j.corsci.2008.09.029
31. Cornell. J.A. Experiments with Mixtures: Designs, Models and the Analysis of Mixture Data, 3rd ed., Wiley, 2002.
32. Montgomery DC. Design and Analysis of Experiments, 7th ed. John Wiley and Sons, 2008.
33. Schlesinger M, Paunovic M. Modern Electroplating, Fourth ed. Joun Willy and Sons, New York, 2000.
34. Mosavat SH, Bahrololoom ME, Shariat MH. Electrodeposition of nanocrystalline Zn–Ni alloy from alkaline glycinate bath containing saccharin as additive. Appl Surf Sci. 2011;257:8311-8316. https://doi.org/10.1016/j.apsusc.2011.03.017
35. Barceló G, García E, Sarret M et al. Characterization of zinc–nickel alloys obtained from an industrial chloride bath. J Appl Electrochem.1998;28:1113-1120. https://doi.org/10.1023/A:1003461109203
36. Feng Z, Li Q, Zhang J et al. Electrodeposition of nanocrystalline Zn-Ni coatings with single gamma phase from an alkaline bath. Surf Coat Technol. 2015;270:47-56. https://doi.org/10.1016/j.surfcoat.2015.03.020
37. Riastuti R, Siallagan ST, Rifki A et al. The effect of saccharin addition to nickel electroplating on the formation of nanocrystalline nickel deposits. IOP Conf Ser Mat Sci Eng. 2019;541:012053. https://doi.org/10.1088/1757-899X/541/1/012053
38. Othman IS, Azam MAFMM, Shafie M et al. Influence of saccharin content on the characteristics and hardness properties of electrodeposited nickel-quarry dust composite coatings. Proceed Mech Eng Res Day. 2020;93(4):357-358.
39. Fabri MFJ, Barcia OE, Diaz SL et al. Electrodeposition of Zn-Ni alloys in sulfate electrolytes. Electrochim Acta. 1996;41:1041-1049. https://doi.org/10.1016/0013-4686(95)00436-X